Title	Proviral silencing in embryonic stem cells requires the histone methyltransferase ESET.
Author(s)	Matsui, Toshiyuki; Leung, Danny; Miyashita, Hiroki; Maksakova, Irina A; Miyachi, Hitoshi; Kimura, Hiroshi; Tachibana, Makoto; Lorincz, Matthew C; Shinkai, Yoichi
Citation	Nature (2010), 464(7290): 927-931
Issue Date	2010-02-17
URL	http://hdl.handle.net/2433/112675
Right	© 2010 Nature Publishing Group
Type	Journal Article
Textversion	author

Proviral silencing in embryonic stem cells requires the histone methyltransferase ESET

Toshiyuki Matsui[1,2*], Danny Leung[3*], Hiroki Miyashita[1,2], Irina A. Maksakova[3], Hitoshi Miyachi[1], Hiroshi Kimura[4], Makoto Tachibana[1,2], Matthew C. Lorincz[3], Yoichi Shinkai[1,2]

[1]Experimental Research Center for Infectious Diseases, Institute for Virus Research, and [2]Graduate School of Biostudies, Kyoto University, 53 Shogoin, Kawara-cho, Sakyo-ku, Kyoto, Japan, [3]Department of Medical Genetics, Life Sciences Institute, The University of British Columbia, Vancouver, British Columbia, Canada, [4]Graduate School of Frontier Biosciences, Osaka University, Suita, Osaka 565-0871, Japan

[#]These authors contributed equally to this work'

Endogenous retroviruses (ERVs), retrovirus-like elements with long terminal repeats, are widely dispersed in the euchromatic compartment in mammalian cells, comprising ~10% of the mouse genome[1]. These parasitic elements are responsible for >10% of spontaneous mutations[2]. Whereas DNA methylation has an important role in proviral silencing in somatic and germ-lineage cells[3–5], an additional DNA-methylation-independent pathway also functions in embryonal carcinoma and embryonic stem (ES) cells to inhibit transcription of the exogenous gammaretrovirus murine leukaemia virus (MLV)[6–8]. Notably, a recent genome-wide study revealed that ERVs are also marked by histone H3 lysine 9 trimethylation (H3K9me3) and H4K20me3 in ES cells but not in mouse embryonic fibroblasts[9]. However, the role that these marks have in proviral silencing remains unexplored. Here we show that the H3K9 methyltransferase ESET (also called SETDB1 or KMT1E) and the Kru¨ppel-associated box (KRAB)-associated protein 1 (KAP1, also called TRIM28)[10,11] are required for H3K9me3 and silencing of

endogenous and introduced retroviruses specifically in mouse ES cells. Furthermore, whereas ESET enzymatic activity is crucial for HP1 binding and efficient proviral silencing, the H4K20 methyltransferases Suv420h1 and Suv420h2 are dispensable for silencing. Notably, in DNA methyltransferase triple knockout (*Dnmt1*$^{-/-}$*Dnmt3a*$^{-/-}$*Dnmt3b*$^{-/-}$) mouse ES cells, ESET and KAP1 binding and ESET-mediated H3K9me3 are maintained and ERVs are minimally derepressed. We propose that a DNA-methylation-independent pathway involving KAP1 and ESET/ESET-mediated H3K9me3 is required for proviral silencing during the period early in embryogenesis when DNA methylation is dynamically reprogrammed.

We recently demonstrated that whereas ES cells lacking the H3K9-specific lysine methyltransferases (KMTases) G9a or GLP show decreased H3K9me2 and DNA methylation of class I and class II ERVs, these elements show no decrease in H3K9me3 and remain transcriptionally silent[12], indicating that deposition of the H3K9me3 mark by an alternative H3K9 KMTase may be essential for silencing of long terminal repeat (LTR) retroelements in ES cells. However, ES cells lacking the H3K9 KMTases Suv39h1 and Suv39h2 (*Suv39h1*$^{-/-}$*Suv39h2*$^{-/-}$)[13], which are responsible for H3K9me3 of pericentromeric heterochromatin, also show no reduction of H3K9me3 at intracisternal A particle (IAP) ERVs and only modest reactivation of these elements[14], implicating an alternative H3K9 KMTase in this process.

To test whether ESET, the remaining member of the Suv39 family of H3K9 KMTases with bona fide catalytic activity, has a role in silencing of ERVs and/or exogenous retroviruses, we generated an *Eset* conditional knockout (CKO) mouse ES cell line, termed 33#6 (Supplementary Figs 2 and 3). 33#6 shows a growth defect after 4-hydroxytamoxifen (OHT)-mediated ESET depletion and modest reduction of total H3K9me3, but not H3K9me2 (Supplementary Figs 4 and 5). Notably, northern blot analysis of these cells, in parallel with *G9a* (also called *Ehmt2*) and *GLP* (also called *Ehmt1*) double knockout (*G9a*$^{-/-}$*GLP*$^{-/-}$)[15], *Suv39h1*$^{-/-}$*Suv39h2*$^{-/-}$ (ref. 13) or *Dnmt1*$^{-/-}$*Dnmt3a*$^{-/-}$*Dnmt3b*$^{-/-}$ (ref. 16) mouse ES cells, revealed that transcription of class I (MLV) and class II (IAP and MusD) ERVs was significantly induced upon ESET deletion, whereas transcription levels of

the non-LTR retrotransposon LINE-1 and the class III ERV MTA were only weakly induced (Fig. 1a and Supplementary Fig. 6). Proviral reactivation after ESET deletion was validated by quantitative polymerase chain reaction after reverse transcription (RT–qPCR) of this and additional Eset CKO ES clones established from *Eset* CKO embryos (Supplementary Fig. 7). In contrast, no increase in ERV expression was observed in *G9a*$^{-/-}$*GLP*$^{-/-}$ or *Suv39h1*$^{-/-}$*Suv39h2*$^{-/-}$ ES cells (Fig. 1a), consistent with our previous observations[12]. Sequence analysis of the MusD elements expressed in 33#6 before and after ESET depletion revealed a higher degree of sequence diversity in the latter, indicating that additional MusD ERVs are reactivated upon ESET deletion (Supplementary Fig. 8). However, comparison to the genomic sequences of all MusD elements reveals that the expressed MusD elements show highest homology to relatively recent insertions, consistent with the observation that mutations in the LTR region of older retroelements reduces their transcription potential[17].

To study the role of ESET in proviral silencing in differentiated cells, we analysed *Eset* heterozygous (+/CKOΔ) and *Eset* null (CKOΔ/CKOΔ) immortalizedmouse embryonic fibroblasts (MEFs) established from *Eset* CKO embryos (Supplementary Fig. 2b, c). In *Eset* null MEFs, IAP, MusD and LINE-1 elements were not derepressed, but MLV expression was significantly induced, even though MLV expression was already higher in MEFs than ES cells (Fig. 1a). Collectively, these findings indicate that although ESET has an important role in the silencing of ERVs in ES cells, this H3K9 KMTase is not generally required for proviral silencing in MEFs.

To determine whether ESET is specifically targeted to class I and class II ERVs, 33#6, 33#6 expressing exogenous ESET (33#6^{TG+}), *Dnmt1*$^{-/-}$*Dnmt3a*$^{-/-}$*Dnmt3b*$^{-/-}$ ES cells and *Eset* heterozygous or null MEFs were analysed via chromatin immunoprecipitation (ChIP). ESET showed a higher level of enrichment on IAP, MusD and MLV ERVs than MTA, major satellite or LINE-1 repeats in ES cells but no enrichment in MEFs (Fig. 1b). ESET enrichment at these ERVs was lost after *Eset* deletion. Furthermore, ESET-dependent H3K9me3 was detected on IAP, MusD and MLV ERVs in 33#6, but not in heterozygous MEFs, consistent with a recent report[9].

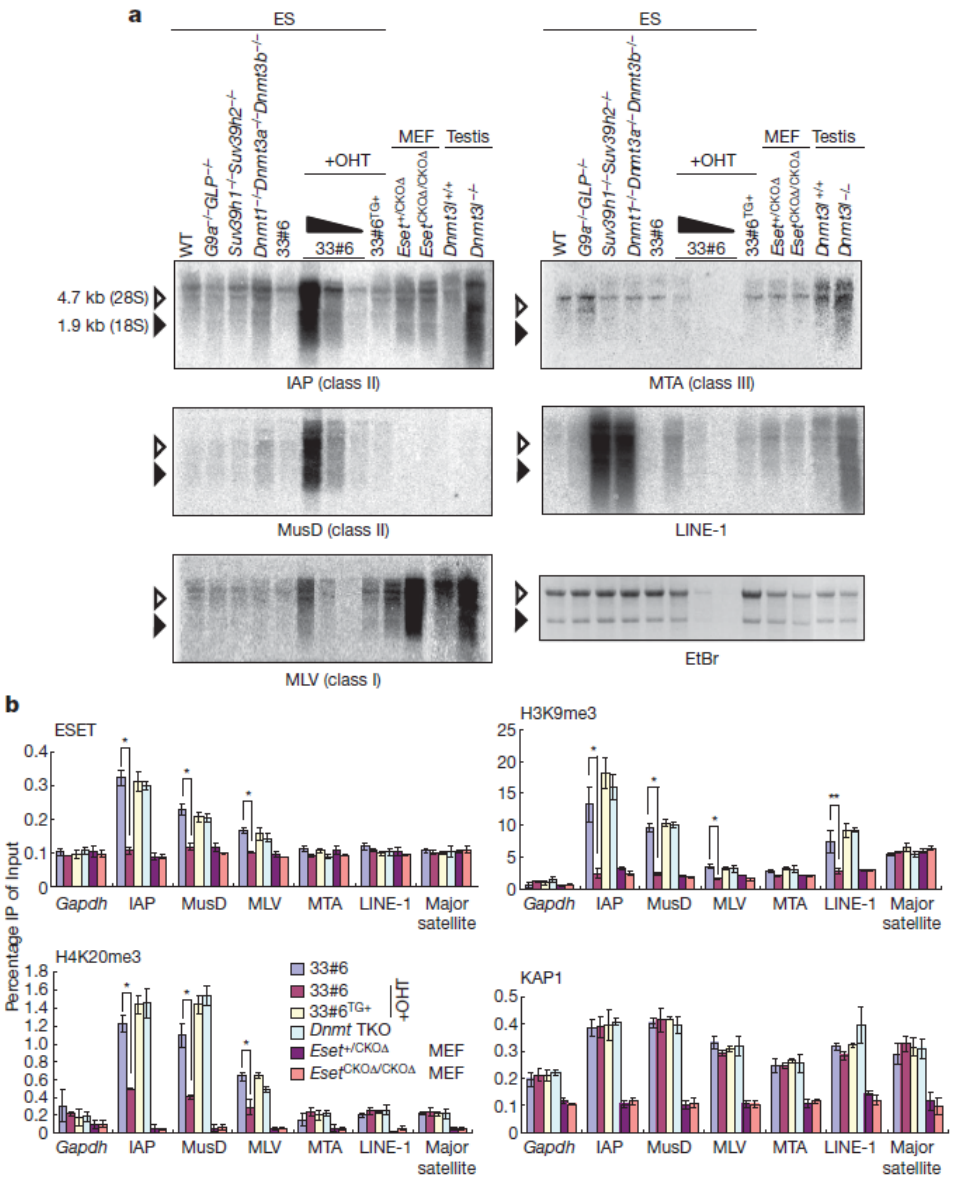

Figure 1 | ESET is required for silencing, H3K9me3 andH4K20me3 of class I and II ERVs in ES cells. a, Northern blot analysis of IAP, MusD, MLV, MTA and LINE-1 expression. Total RNA was isolated from wild-type, *G9a*$^{-/-}$*GLP*$^{-/-}$, *Suv39h1*$^{-/-}$*Suv39h2*$^{-/-}$, *Dnmt1*$^{-/-}$*Dnmt3a*$^{-/-}$ *Dnmt3b*$^{-/-}$, *Eset* CKO (33#6), 33#6 treated with OHT (33#6^{TG+}OHT) and 33#6 stably expressing exogenous ESET treated with OHT (33#6^{TG+} +OHT) ES cells, *Eset*$^{+/-}$ and *Eset*$^{-/-}$ MEFs and testes isolated from *Dnmt3l*$^{-/-}$ or *Dnmt3l*$^{-/-}$ mice. The integrity of these RNA samples was validated by ethidium bromide (EtBr) staining and the absence of genomic DNA contamination was confirmed by treating the 33#6 +OHT sample with RNase, which

eliminated the IAP signal (Supplementary Fig. 6). Four micrograms total RNA was loaded per lane except for 33#6 +OHT (4 mg and 1/5 serial dilution). IAP IΔ1 transcripts and full-length A type LINE-1 elements are ,5.4 and , 7 kb, respectively. b, Chromatin was isolated from 33#6, 33#6 +OHT, 33#6^{TG+} +OHT or *Dnmt1*$^{-/-}$*Dnmt3a*$^{-/-}$*Dnmt3b*$^{-/-}$ (Dnmt TKO) ES cells and from *Eset*$^{+/-}$ or *Eset*$^{-/-}$ MEFs. ChIP–qPCR analysis was conducted using ESET-, H3K9me3-, H4K20me3- and KAP1- specific antibodies and primers specific for IAP, MusD, MLV, MTA, LINE-1 and major satellite repeats and the Gapdh gene. Graphs show the mean ChIP enrichment values (n = 3, technical replicates) with s.d. (error bars). A representative experiment is shown. As no enrichment of ESET, H3K9me3 or H4K20me3 was detected with MLV-specific primers in MEFs, the induction of MLV transcripts observed on ESET depletion in these cells is probably an indirect effect. *P < 0.005, **P < 0.05 (Student's t-test).

In contrast, H3K9me2 showed either a modest increase (at IAP) or no significant change (at MusD and MLV ERVs) after ESET depletion (Supplementary Fig. 9), indicating that ESET is not responsible for deposition of this mark in vivo[12]. ESET and H3K9me3 were also detected in regions 3' of the 5' LTR of each ERV analysed and H3K9me3 in these distal regions was lost on ESET deletion (Supplementary Fig. 9).

Consistent with previous reports[9,14], ERVs also showed H4K20me3 enrichment in ES cells (Fig. 1b). This mark was significantly reduced after *Eset* deletion, indicating that ESET acts upstream of the KMTases Suv420h1 and Suv420h2, which are responsible for deposition of the H4K20me3 mark[18]. H3K9me3 may generally be required for H4K20me3 deposition, as Suv39h1 and Suv39h2 act upstream of Suv420h1 and Suv420h2 at major satellite repeats[18,19]. Notably, whereas enrichment of H4K20me3 was lost at IAP, MusD and MLV ERVs in *Suv420h1*$^{-/-}$*Suv420h2*$^{-/-}$ cells, enrichment of H3K9me3 was unperturbed (Supplementary Fig. 10) and no increase in ERV expression was detected (Supplementary Fig. 11), indicating that ESET-mediated ERV silencing does not depend on Suv420h1 and Suv420h2 or H4K20me3.

ESET interacts in a large co-repressor complex that includes KAP1 (ref. 20), HP1 proteins[21] and subunits of a NuRD-like complex[22]. Intriguingly, a complex including KAP1 and the KRAB zinc finger protein (ZFP) ZFP809 was recently shown to bind to an ecotropic MLV-based vector bearing a primer binding site (PBS) complementary to proline tRNA (PBS^{Pro}), and to silence this provirus in embryonal carcinoma cells[10,11]. The PBS region is also required for silencing of MLV in the early embryo[23]. However, ZFP809 does not repress related PBS^{Gln} proviruses[11], such as the polytropic MLV ERV studied here. Similarly, IAP and MusD ERVs, which use PBSs complementary to $tRNA^{Phe}$ and $tRNA^{Lys3}$, respectively, are unlikely to be silenced by ZFP809. Thus, ESET-mediated silencing of these proviruses may be mediated by alternative KRAB ZFPs[24], or an alternative silencing pathway, such as via an interaction with MBD1 (ref. 25).

To determine whether ERVs are bound by KAP1, ES cells and MEFs were analysed via ChIP. KAP1 enrichment was detected in the LTR and downstream regions in ES cells, but not in MEFs (Fig. 1b and Supplementary Fig. 9). ESET depletion did not affect KAP1 expression (Supplementary Fig. 2c) or recruitment at any of the regions surveyed. To

determine whether KAP1 or MBD1 are required for proviral silencing, we used short interfering RNAs (siRNAs) to knockdown ESET, KAP1 or MBD1. As observed for ESET knockdown, KAP1 knockdown yielded a marked increase in proviral expression (Supplementary Fig. 12a) and a concomitant decrease in ESET binding and H3K9me3 at these elements (Supplementary Fig. 12b). In contrast, depletion of MBD1 yielded no increase in ERV expression, despite efficient knockdown. Taken together, these results indicate that KAP1 acts upstream of ESET in a proviral silencing pathway.

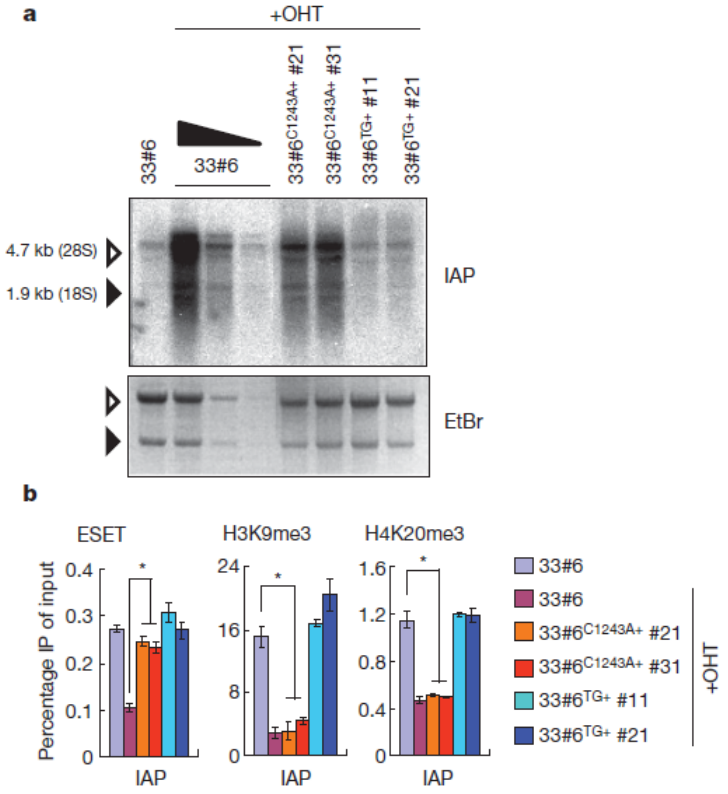

Figure 2 | Intrinsic KMTase activity is crucial for ESET-mediated ERV silencing. a, Northern blot analysis of 33#6, 33#6 expressing wild-type ESET (33#6^{TG+}) or a KMTase-defective mutant (C1243A) of ESET (33#6$^{C1243A+}$) was conducted, as in Fig. 1a. Expression of wild-type ESET and ESET(C1243A) was validated by western blot analysis shown in Supplementary Fig. 3b. b, ChIP–qPCR analysis of H3K9me3, H4K20me3 and ESET in 33#6, 33#6^{TG+} and 33#6$^{C1243A+}$ lines before and after ESET deletion. Graphs show the mean ChIP enrichment values (n = 3, technical replicates) with s.d. (error bars). Statistical comparisons were conducted between 33#6 and 33#6$^{C1243A+}$ +OHT lines (H3K9me3 and H4K20me3) or 33#6 +OHT and 33#6$^{C1243A+}$ +OHT lines (ESET).

Next, we addressed whether ESET-mediated ERV silencing requires intrinsic KMTase activity. Substitution of amino acid 1228 (C1228A) of human ESET (corresponding to Cys 1243 of mouse ESET) markedly reduces the KMTase activity of this enzyme[20]. A KMTase-defective ESET(C1243A) transgene (Supplementary Fig. 3) suppressed IAP reactivation less efficiently than wild-type ESET after ESET depletion (Fig. 2a, ,25-fold, ,10-fold and no induction in 33#6, 33#6$^{C1243A+}$ and 33#6^{TG+}, respectively) and did not rescue the growth defect phenotype (Supplementary Fig. 4). Furthermore, reduction of H3K9me3 and H4K20me3 was not complemented by the ESET(C1243A) transgene (Fig. 2b). Taken together, these results indicate that although ESET is associated with a modest KMTase independent repression activity, intrinsic KMTase activity is critical for efficient ESET-dependent ERV silencing and cell growth/viability in ES cells.

Given that HP1 proteins, which are known to have a role in transcriptional silencing, interact with H3 methylated on K9 (ref. 26), we next conducted ChIP using antibodies specific for HP1α, HP1β and HP1γ. Whereas a decrease in enrichment of all three proteins was clearly observed in ESET-depleted cells in the promoter and downstream regions of IAP, MusD and MLV ERVs (Supplementary Fig. 13), HP1α and HP1γ were not reduced to background levels. Residual HP1 recruitment could be due to the persistence of H3K9me2, an H3K9-methylation-independent interaction with nucleosomes, or direct interaction with KAP1 (ref. 21).

Surprisingly, ERVs are derepressed to a lesser extent in *Dnmt1*$^{-/-}$ *Dnmt3a*$^{-/-}$*Dnmt3b*$^{-/-}$ ES cells than ESET knockout ES cells (Fig. 1a). Furthermore, ESET, H3K9me3 and H4K20me3 enrichment at these elements is maintained in *Dnmt1*$^{-/-}$*Dnmt3a*$^{-/-}$*Dnmt3b*$^{-/-}$ ES cells (Fig. 1b), indicating that ESET targeting and deposition of ESET-associated histone marks occurs independently of DNA methylation. To determine whether ESET is required for DNA methylation of ERVs, we analysed the DNA methylation states of the promoter regions of these elements before and after ESET depletion (Fig. 3). The percentage of methylated CpGs was either unchanged for IAP elements (91.3% before versus 91.1% after) or moderately decreased for MLV and MusD ERVs (95.6% before versus 65.5% after and 82.6% before versus 61.9% after, respectively). Methylation-sensitive Southern blotting revealed a similar pattern

(Supplementary Fig. 14). Thus, ESET is not essential for DNA methylation of ERVs per se. As only a subset of IAP, MusD or MLV ERVs— of which there are ~2,500, ~110 and ~50 copies in the mouse genome, respectively—are potentially active (a relatively high GC→AT transition rate[27] reduces the transcription efficiency of 'older' elements[17]), it is possible that the DNA demethylation observed occurs specifically at 'young' ERVs that are derepressed after ESET depletion. However, determining the DNA methylation states specifically of the proviruses that are derepressed on ESET depletion is technically challenging.

To circumvent this problem, we chose to study the murine stem cell virus (MSCV; Fig. 4a), an MLV-based exogenous retrovirus with a strong enhancer/promoter that nevertheless is frequently silenced in ES cells early after infection via a DNA-methylation-independent pathway[8]. ChIP analysis of J1 wild-type and *Dnmt1*$^{-/-}$*Dnmt3a*$^{-/-}$*Dnmt3b*$^{-/-}$ ES cells revealed significant enrichment of H3K9me3 at the MSCV provirus in both lines at day 4 after infection, indicating that this mark is deposited at newly integrated exogenous retroviruses in a DNA-methylation-independent manner (Fig. 4b). Furthermore, the provirus shows minimal de novo DNA methylation in wild-type J1 cells at this time point[7]. To determine whether ESET is required for silencing of the MSCV provirus, 33#6 and 33#6^{TG+} cells were infected with MSCV–GFP, and GFP-negative cells were isolated at day 14 after infection (Supplementary Fig. 15). This population of cells, which includes both uninfected cells and cells harbouring silent provirus (with a mean proviral copy number of 0.86 copies per cell), was expanded for further analyses. After ESET deletion, the percentage of viable GFP^{+} 33#6 cells increased markedly (Fig. 4c), as did the level of proviral RNA (Supplementary Fig. 16). H3K9me3 and H4K20me3 enrichment across the MSCV provirus was concomitantly reduced, whereas H3K9me2 levels remained unchanged (Fig. 4d). Furthermore, knockdown of KAP1 also yielded a significant increase in expression of the MSCV provirus in addition to loss of H3K9me3 and ESET binding (Supplementary Fig. 17). Thus, as for ERVs, ESET-mediated silencing of MLV-based exogenous retroviruses in ES cells is dependent on KAP1 (refs 10, 11).

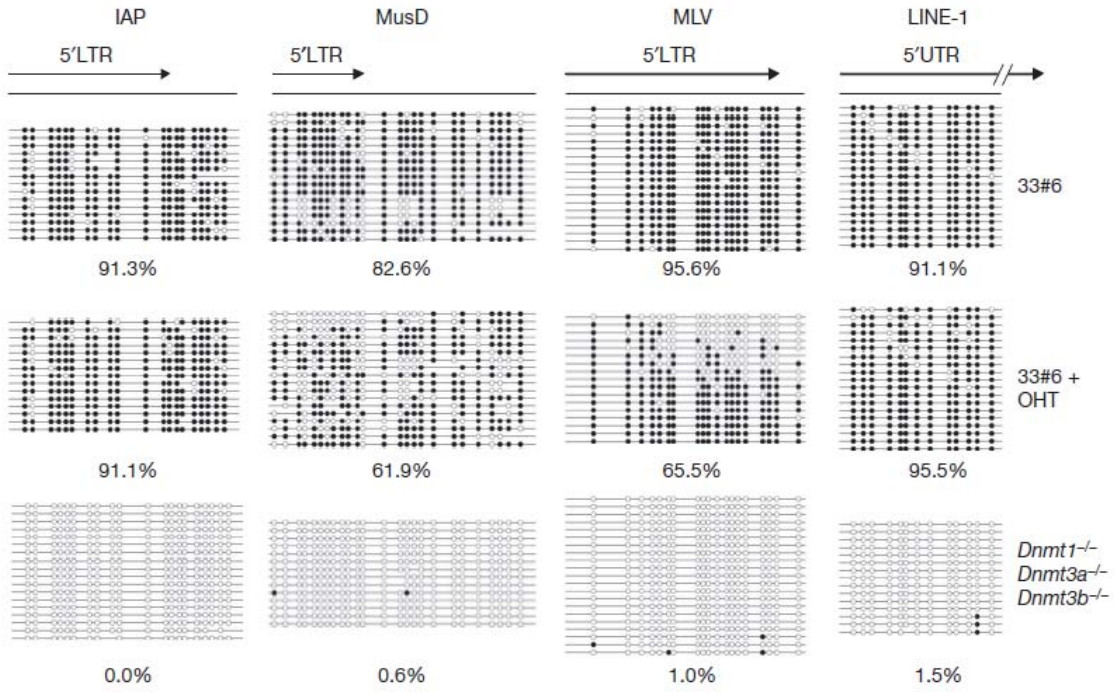

Figure 3 | Deletion of ESET does not lead to global DNA demethylation of ERVs. Bisulphite sequencing analysis of IAP,MusDandMLVERVs andLINE-1 non-LTR retroelements was conducted on genomic DNA isolated from 33#6, 33#6 +OHT and *Dnmt1*$^{-/-}$*Dnmt3a*$^{-/-}$*Dnmt3b*$^{-/-}$ ES cells. Open and filled circles represent unmethylated or methylated cytosines, respectively. The percentage of total methylated CpGs/CpGs is presented below each data set.

To determine whether derepression of the MSCV provirus is accompanied by DNA demethylation, uninduced cells or GFP^{+} cells sorted at day 6 after OHT addition were analysed by bisulphate sequencing. Whereas the 5' LTR was densely methylated before OHT treatment (Fig. 4e), the sorted/GFP^{+} population showed a significantly lower level of DNA methylation in this region, indicating that reactivation of proviral expression after ESET depletion is frequently accompanied by loss of DNA methylation.

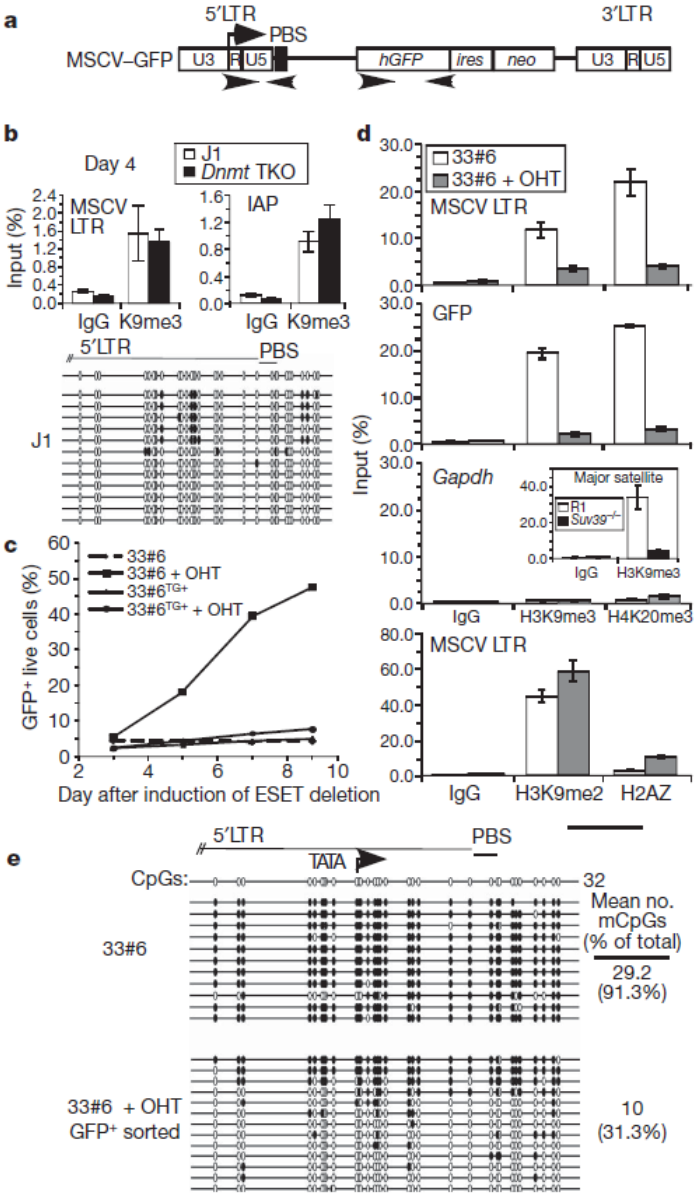

Figure 4 | Derepression of exogenous retrovirus expression on Eset depletion is accompanied by reduced levels of proviral H3K9me3 and DNA methylation. a, A map of the MSCV–GFP (PBS^{Gln}) provirus and amplicons used for ChIP are shown. b, Wild-type J1 and *Dnmt1*$^{-/-}$*Dnmt3a*$^{-/-}$ *Dnmt3b*$^{-/-}$ cells were infected with MSCV–GFP and chromatin was isolated at day 4 after infection. ChIP was conducted with antibodies specific for H3K9me3 or non-specific IgG as a control. Enrichment was analysed by qPCR with primers specific for the MSCV or IAP LTR regions. Genomic DNA was collected on the same day from J1 cells for bisulphite analysis of

the MSCV 5' LTR. All ChIP–qPCR graphs show the mean ChIP enrichment values (n = 3, technical replicates) with s.d. (error bars). c, 33#6 or 33#6^{TG+} cells were infected with MSCV–GFP and pools of cells harbouring silent proviruses (GFP$^-$) were isolated by FACS (see Supplementary Fig. 15). These GFP$^-$ cells were treated with OHT to induce Eset deletion and viable cells were analysed by flow cytometry at days 3, 5, 7 and 9 after OHT treatment. d, Chromatin was isolated from the pool of infected 33#6 cells, either untreated or OHT treated and ChIP was conducted with antibodies specific for H3K9me2, H3K9me3, H4K20me3 and H2AZ. Non-specific IgG was used as a control. The level of enrichment was determined by qPCR using primers specific for the MSCV 5' LTR region or the GFP gene. Gapdh specific primers were used as a negative control. Major satellite specific primers (inset) were used as a positive control with chromatin isolated from R1 wild-type and *Suv39h1*$^{-/-}$*Suv39h2*$^{-/-}$ (Suv39$^{-/-}$) ES cells. e, Genomic DNA was isolated from untreated GFP$^+$ 33#6 cells (>30 days after infection) or GFP$^+$ cells sorted from this pool at day 6 after OHT treatment and analysed by bisulphite sequencing as in b. Locations of the TATA box, 5' LTR and PBS are shown. Open and filled circles represent unmethylated or methylated cytosines, respectively.

Our observations reveal that ESET is a critical downstream effector of a KAP1-dependent silencing pathway that acts on ERVs as well as exogenous retroviruses in ES cells (Supplementary Fig. 1). Why ESET is required for silencing of proviral elements specifically in ES cells, where they are generally densely DNA methylated, remains unclear. DNAmethylation may not efficiently mediate silencing of ERVs in ES cells as a result of high turnover or the absence of co-repressors, such as MBD proteins.

ERVs are variably demethylated early in embryogenesis and in primordial germ cells, in conjunction with the genome-wide demethylation that occurs at these stages[28,29]. Given that ESET is expressed at high levels in oocytes and pre-implantation embryos[30] and is required for deposition of the H3K9me3 mark at MLV, IAP and MusD retroelements, we propose that this KMTase has a critical role in silencing of such ERVs specifically during those stages in development when DNA methylation is

reprogrammed.

METHODS SUMMARY

Generation of *Eset* CKO ES cells, mice and MEFs. *Eset* CKO ES cells were established by standard gene targeting procedures, as summarized in Supplementary Fig. 1a. Once a clone containing targeted *Eset* CKO and knockout alleles was established (#32), we introduced a vector expressing the Cre- oestrogen receptor fusion gene Mer-Cre-Mer to generate the *Eset* CKO ES cell line, 33#6. An *Eset* CKO mouse line was established from the first targeted ES cell clone possessing the CKO allele (3-6-5) and crossed with B6.Cg-Tg(Cre/Esr1)5Amc/J mice ubiquitously expressing Cre/Esr1 (The Jackson Laboratory, 004682). *Eset* CKO MEFs were prepared from E13.5 $Eset^{CKO/CKO}$ or $Eset^{CKO/+}$, cre/$Esr1^{TG+}$ embryos and immortalized with large-T antigen. After immortalization, Eset deletion was induced by OHT treatment to generate *Eset* knockout MEFs.

Northern blot analysis. Total RNA was isolated with Sepasol-RNA I (Nacalai Tesque) and treated with Recombinant DNase I (10 mg total RNA per 1 unit; RNase-free, TAKARA) at 37 ^{o}C for 2 h. Probes were generated using primers shown in Supplementary Table 1.

Bisulphite sequencing analysis. Bisulphite sequencing was conducted using the EZ DNA Methylation-Gold kit (Zymo Research) or EpiTech bisulphite Kit (Qiagen), as previously described[12]. PCR products were cloned and individual inserts were sequenced using BigDye v3.1 chemistry. Sequencing datawas analysed using Sequencher software (Gene Codes) or QUMA (http://quma.cdb.riken.jp/).

Further protocols. Detailed protocols of siRNA-mediated knockdown, ChIP, RT–qPCR, Southern and western analyses and cell culture conditions are provided in the Methods.

Full Methods and any associated references are available in the online version of the paper at www.nature.com/nature.

Received 10 August 2009; accepted 16 January 2010.

Published online 17 February; corrected 8 April 2010 (see full-text HTML version for details).

1. Mouse Genome Sequencing Consortium. Initial sequencing and comparative analysis of the mouse genome. Nature 420, 520–562 (2002).
2. Maksakova, I. A. et al. Retroviral elements and their hosts: insertional mutagenesis in the mouse germ line. PLoS Genet. 2, e2 (2006).
3. Walsh, C. P., Chaillet, J. R. & Bestor, T. H. Transcription of IAP endogenous retroviruses is constrained by cytosinemethylation. Nature Genet. 20, 116–117(1998).
4. Yoder, J. A., Walsh, C. P. & Bestor, T. H. Cytosine methylation and the ecology of intragenomic parasites. Trends Genet. 13, 335–340 (1997).
5. Bourc'his, D.&Bestor, T. H. Meiotic catastrophe and retrotransposon reactivation in male germ cells lacking Dnmt3L. Nature 431, 96–99 (2004).
6. Teich, N. M., Weiss, R. A., Martin, G. R. & Lowy, D. R. Virus infection of murine teratocarcinoma stem cell lines. Cell 12, 973–982 (1977).
7. Niwa, O., Yokota, Y., Ishida, H. & Sugahara, T. Independent mechanisms involved in suppression of the Moloney leukemia virus genome during differentiation of murine teratocarcinoma cells. Cell 32, 1105–1113 (1983).
8. Pannell, D. et al. Retrovirus vector silencing is de novo methylase independent and marked by a repressive histone code. EMBO J. 19, 5884–5894 (2000).
9. Mikkelsen, T. S. et al. Genome-wide maps of chromatin state in pluripotent and lineage-committed cells. Nature 448, 553–560 (2007).
10. Wolf, D. & Goff, S. P. TRIM28 mediates primer binding site-targeted silencing of murine leukemia virus in embryonic cells. Cell 131, 46–57 (2007).
11. Wolf, D.&Goff, S. P. Embryonic stem cells use ZFP809 to silence retroviral DNAs. Nature 458, 1201–1204 (2009).
12. Dong, K. B. et al.DNAmethylation in ES cells requires the lysine methyltransferase G9a but not its catalytic activity. EMBO J. 27, 2691–2701 (2008).
13. Peters, A. H. et al. Partitioning and plasticity of repressive histone methylation states in mammalian chromatin. Mol. Cell 12, 1577–1589 (2003).

14. Martens, J. H. et al. The profile of repeat-associated histone lysine methylation states in the mouse epigenome. EMBO J. 24, 800–812 (2005).
15. Tachibana, M. et al. Histone methyltransferases G9a and GLP form heteromeric complexes and are both crucial for methylation of euchromatin at H3-K9. Genes Dev. 19, 815–826 (2005).
16. Tsumura, A. et al. Maintenance of self-renewal ability of mouse embryonic stem cells in the absence of DNA methyltransferases Dnmt1, Dnmt3a and Dnmt3b. Genes Cells 11, 805–814 (2006).
17. Maksakova, I. A. & Mager, D. L. Transcriptional regulation of early transposon elements, an active family of mouse long terminal repeat retrotransposons. J. Virol. 79, 13865–13874 (2005).
18. Schotta, G. et al. A silencing pathway to induce H3-K9 and H4-K20 trimethylation at constitutive heterochromatin. Genes Dev. 18, 1251–1262 (2004).
19. Kourmouli, N. et al. Heterochromatin and tri-methylated lysine 20 of histone H4 in animals. J. Cell Sci. 117, 2491–2501 (2004).
20. Schultz, D. C., Ayyanathan, K., Negorev, D., Maul, G. G. & Rauscher, F. J. III. SETDB1: a novel KAP-1-associated histone H3, lysine 9-specific methyltransferase that contributes to HP1-mediated silencing of euchromatic genes by KRAB zinc-finger proteins. Genes Dev. 16, 919–932 (2002).
21. Ryan, R. F. et al. KAP-1 corepressor protein interacts and colocalizes with heterochromatic and euchromatic HP1 proteins: a potential role for Kruppelassociated box-zinc finger proteins in heterochromatin-mediated gene silencing. Mol. Cell. Biol. 19, 4366–4378 (1999).
22. Schultz, D. C., Friedman, J. R. & Rauscher, F. J. III. Targeting histone deacetylase complexes via KRAB-zinc finger proteins: the PHD and bromodomains of KAP-1 form a cooperative unit that recruits a novel isoform of the Mi-2a subunit of NuRD. Genes Dev. 15, 428–443 (2001).
23. Vernet, M. & Cebrian, J. cis-acting elements that mediate the negative regulation of Moloney murine leukemia virus in mouse early embryos. J. Virol. 70, 5630–5633 (1996).
24. Wolf, D., Hug, K. & Goff, S. P. TRIM28 mediates primer binding site-targeted silencing of Lys1,2 tRNA-utilizing retroviruses in embryonic cells. Proc. Natl Acad. Sci. USA 105, 12521–12526 (2008).
25. Sarraf, S. A.&Stancheva, I. Methyl-CpG binding protein MBD1

couples histone H3 methylation at lysine 9 by SETDB1 to DNA replication and chromatin assembly. Mol. Cell 15, 595–605 (2004).
26. Lachner, M., O'Carroll, D., Rea, S., Mechtler, K. & Jenuwein, T. Methylation of histone H3 lysine 9 creates a binding site for HP1 proteins. Nature 410, 116–120 (2001).
27. Meunier, J., Khelifi, A., Navratil, V. & Duret, L. Homology-dependent methylation in primate repetitive DNA. Proc. Natl Acad. Sci. USA 102, 5471–5476 (2005).
28. Kim, S. H. et al. Differential DNA methylation reprogramming of various repetitive sequences in mouse preimplantation embryos. Biochem. Biophys. Res. Commun. 324, 58–63 (2004).
29. Lane, N. et al. Resistance of IAPs to methylation reprogramming may provide a mechanism for epigenetic inheritance in the mouse. Genesis 35, 88–93 (2003).
30. Dodge, J. E., Kang, Y. K., Beppu, H., Lei, H. & Li, E. Histone H3-K9 methyltransferase ESET is essential for early development. Mol. Cell. Biol. 24, 2478–2486 (2004).

Supplementary Information is linked to the online version of the paper at www.nature.com/nature.

Acknowledgements We thank M. Okano for *Dnmt1*$^{-/-}$*Dnmt3a*$^{-/-}$*Dnmt3b*$^{-/-}$ ES cells; T. Jenuwein and P. Singh for *Suv39h1*$^{-/-}$*Suv39h2*$^{-/-}$ ES cells; T. Jenuwein and G. Schotta for *Suv420h1*$^{-/-}$*Suv420h2*$^{-/-}$ ES cells; K. Hata for *Dnmt3l* knockout mice testes; M. Hijikata for the large-T antigen expression vector; S. Kuramochi-Miyagawa for IAP and LINE-1 probes; S. Smale for HP1α antiserum; and L. Gaudreau for H2AZ antiserum. We are also grateful to P. Goyal and members of the Shinkai laboratory for technical support and D. Mager for critically reading the manuscript. This work was supported in part by the Genome Network Project from the Ministry of Education, Culture, Sports, Science and Technology (MEXT) of Japan, Grants-in-aid from MEXT to Y.S. and CIHR grants 77805 and 92090 to M.C.L. M.C.L. is a Scholar of the Michael Smith Foundation for Health Research.

Author Contributions T.M. and D.L. are equally contributing first

authors; M.C.L. and Y.S. are eqully contributing senior authors. Y.S., M.C.L., D.L. and T.M. planned studies and interpreted the data. T.M. validated the *Eset* CKO lines and performed most of the ERV-related studies. D.L. performed the siRNA and exogenous retrovirus-related experiments. H. Miyashita generated *Eset* CKO ES cells and mice. I.A.M. conducted the MusD sequencing analysis. H. Miyachi injected *Eset* CKO ES cells into blastocysts to make chimaeric mice. H.K. provided antibodies against methylated histones. M.T. cloned mouse *Eset* cDNA and provided his expertise in most of the studies conducted in this work. Y.S., M.C.L., D.L. and T.M. wrote the paper.

Author Information Reprints and permissions information is available at www.nature.com/reprints. The authors declare no competing financial interests. Correspondence and requests for materials should be addressed to Y.S. (yshinkai@virus.kyoto-u.ac.jp) or M.C.L. (mlorincz@interchange.ubc.ca).

METHODS

Cell culture. ES cells were maintained in Dulbecco's modified Eagle's medium(Sigma) containing 10% Knockout SR (Invitrogen), 1% fetal calf serum, leukaemia-inhibiting factor, penicillin/streptomycin, L-glutamine, non-essential amino acids and β-mercaptoethanol (ES medium). To generate ES cells stably expressing ESET or ESET(C1243A), expression vectors, pCAG-3XFlag-ESETIRESbsd, were introduced into *Eset* CKO ES cells via Lipofectamine2000 (Invitrogen). Clones were selected in ES medium containing blasticidin (7 μg ml^{-1}). ES cells were cultured in ES medium with 800nM OHT for 4 days, and further cultured without OHT for 2 days to induce deletion of the *Eset* CKO allele.

Immunofluorescence analysis. Cytospun cells were fixed with 4% paraformaldehyde for 10 min at room temperature, permeabilized with 1% Triton X-100 for 10 min, and incubated overnight with primary antibodies (4 ^{o}C). Anti-mouse IgG conjugated with Zenon Alexa-568 Fluor (Molecular Probes) were used as secondary antibodies. The nuclei were counterstained with DAPI, observed under fluorescence microscopy, and analysed with AxioVision software (Zeiss).

RT–qPCR. RNA was isolated as mentioned and qPCR was carried out

using SYBR Premix Ex TaqII (TAKARA) on the ABI7500 Real-Time PCR system. The signals were standardized on input DNA. For ERV expression assays, RT–qPCR was performed using M-MuLV Reverse Transcriptase (Fermentas) and analysed with the same system. The signals were normalized with Gapdh. Primer sequences are shown in Supplementary Table 1.

Cloning of MusD cDNA sequences. RNA was isolated as above from wild-type and *ESET* CKO ES cells 6 days after OHT treatment. RNA was then converted to cDNA using Superscript II according to manufacturer's protocol. PCR was conducted on cDNA samples with primers specific for the MusD 5' LTR and 3' proximal region. The PCR product was resolved on an agarose gel and subsequently extracted with the Qiagen gel extraction kit. The purified product was TA cloned into pGEM-T vector (Promega) and sequenced. Sequences were aligned and phylogenetic trees constructed using MEGA4 software[31].

Viral infections and copy number determination. For infection of target ES cells with MSCV–GFP retrovirus[32], the Phoenix A retroviral expression system was used as previously described[33]. Proviral copy number was determined by qPCR using genomic DNA isolated from infected pools or a control cell line harbouring a single-copy GFP transgene (as determined by Southern blotting) and primers specific for GFP. Samples were normalized to the endogenous β-major gene.

Flow cytometry and cell sorting. Trypsinized cells were resuspended in 500 ml PBS with 2% bovine calf serum and 1 $\mu g\ ml^{-1}$ propidium iodide and analysed with a LSRII flow cytometer (BD). Data on 10,000 viable cells (as determined by electronic gating in the forward and side scatter channels) were collected for each sample and analysed using FlowJo software (Treestar). To generate cells harbouring silent MSCV–GFP proviruses, 33#6 cells were infected with MSCV–GFP retrovirus and GFP-negative cells were isolated by FACS at day 14 after infection. This population was cultured and expanded for further analysis.

Native ChIP and crosslinked ChIP. ERV native and crosslinked ChIP experiments were performed as described previously[34].

Antibodies. Antibodies used for western blotting, immunofluorescence and ChIP include: anti-H3K9me2 (6D11 (ref. 34)), anti-H3K9me3 (2F3 (ref. 4) and Active Motif, 39161), anti-H4K20me3 (27F10 and Active Motif,

39180), anti-KAP1 (Abcam, ab22553), anti-ESET/SETDB1 (Millipore, 07-378), anti- Flag M2 (Sigma, F3165), anti-HP1α (Upstate, 05-689 and 2049; gift from S. Smale), anti-HP1β (AbD SeroTec, MCA1946 and Euromedex, 1MOD-1A9), anti-HP1γ (Upstate, 05-690 and Euromedex, 2Mod-1G6), anti-tubulin (Oncogene, CP-06) and anti-H3 C-terminal (Active Motif, 39163).

Exogenous retrovirus native ChIP. To generate chromatin, 13107 infected ES cells for each cell line were collected and homogenized through a needle syringe. MNase was added to digest chromatin to nucleosome size fragments. The fragmented chromatin is then pre-cleared with protein A and G sepharose beads and immunoprecipitated with antibodies of interest and sepharose beads. The material is then washed, eluted and purified with the Qiagen PCR purification kit. The samples are then analysed by qPCR. Detailed protocol is available on request.

siRNA-mediated knockdown. For knockdown experiments, ES cells were trypsinized, diluted in antibiotic-free ES media, seeded on a 6-well plates (23105 per well) and cultured overnight at 37 ^{o}C. On the day of transfection, stock solutions (20 mM) of siRNAs targeting *Eset*, *Kap1*, *Mbd1* (siGENOME SMARTpool or siGENOME siRNAs) or control (*Psp1*) (59-GGAAGGCUCUUGAUGAAAUGG-39) were diluted to 2 mM with siRNA buffer (Dharmacon). In two separate tubes, 50 ml of 2 mM siRNA was mixed with 50 ml of OPTI-MEM(tube 1) and 4 ml of DharmaFECT transfection reagent 1 was mixed with 96 ml of OPTI-MEM (tube 2). Both tubes were incubated for 5 min at room temperature. Tubes 1 and 2 were then mixed and incubated at 25 ^{o}C for 20 min for the lipid–siRNA complex to form. Fresh antibiotic-free media (1.8 ml) was then mixed with the transfection reagent–siRNA solution and added to the well after growth medium removal. Transfected cells were passaged 24 h after transfection. A second transfection was conducted with the same reagents on the following day.

Transient transfection. Transient transfection was performed in 293T cells using a TransIT-LT1 lipofection reagent (Mirus). For the in vitro HMTase assay, Flag–ESET or Flag–ESET(C1243A) was immunoprecipitated with anti-Flagconjugated Protein G beads 48 h after transfection.

In vitro HMTase assay. The histone methyltransferase assay was

performed as described previously[34]. Ten microlitres of reaction mixture containing recombinant H3 and H4, 50 nCi of S-adenosyl-[methyl-^{14}C]-L-methionine and purified Flag–ESET or Flag–ESET(C1243A) in methylation reaction buffer (50mM Tris, pH 8.5, 20mM KCl, 10mM $MgCl_2$, 10mM β-mercaptoethanol, 250mM sucrose) was incubated for 60 min at 30 ^{o}C. The reaction products were separated by 15% SDS–PAGE. Detection of methyl-^{14}C was performed using a BAS-5000 imaging analyser (Fuji Film).

Whole-cell extraction for western blotting. Briefly, cells were resuspended in 2X Laemmli buffer and incubated at 100 ^{o}C for 10 min. Cells were then homogenized through a 25-gauge needle syringe for 10–15 repetitions. Extract was loaded and run on SDS–PAGE gel as standard protocols.

Methylation-sensitive Southern blot analysis. Genomic DNA was digested overnight with methylation-sensitive restriction enzyme HpaII or methylation- insensitive restriction enzyme MspI. Digests were separated with 0.8% agarose-gel, transferred to a nylon membrane and hybridized with specific probes, generated with primers shown in Supplementary Table 1.

Probes for northern blot analysis. ERV-specific probes were generated using primers described previously[35].

31. Tamura, K.,Dudley, J.,Nei,M.&Kumar, S.MEGA4:Molecular EvolutionaryGenetics Analysis (MEGA) software version 4.0. Mol. Biol. Evol. 24, 1596–1599 (2007).
32. Hawley, R. G., Lieu, F. H., Fong, A. Z. & Hawley, T. S. Versatile retroviral vectors for potential use in gene therapy. Gene Ther. 1, 136–138 (1994).
33. Lorincz, M. C. et al. Dynamic analysis of proviral induction and de novo methylation: implications for a histone deacetylase-independent, methylation density-dependent mechanism of transcriptional repression. Mol. Cell. Biol. 20, 842–850 (2000).
34. Tachibana, M., Matsumura, Y., Fukuda, M., Kimura, H. & Shinkai, Y. G9a/GLP complexes independently mediate H3K9 and DNA methylation to silence transcription. EMBO J. 27, 2681–2690 (2008).
35. Kuramochi-Miyagawa, S. et al. DNA methylation of retrotransposon

genes is regulated by Piwi family members MILI and MIWI2 in murine fetal testes. Genes Dev. 22, 908–917 (2008).